Design and fabrication of a high-performance evanescently coupled waveguide photodetector*

Liu Shao-Qing(刘少卿), Yang Xiao-Hong(杨晓红)†, Liu Yu(刘 宇), Li Bin(李 彬), and Han Qin(韩 勤)‡

State Key Laboratory of Integrated Optoelectronics, Institute of Semiconductors, Chinese Academy of Sciences, Beijing 100083, *China*

(Received 6 February 2013; revised manuscript received 22 March 2013)

In this paper, we present the design, fabrication, and measurement of an evanescently coupled waveguide photodetector operating at 1.55 μm, which mainly comprises a diluted waveguide, a single-mode rib waveguide and a p–i–n photodiode with an extended optical matching layer. The optical characteristics of this structure are studied by using a three-dimensional finite-difference time-domain (3D FDTD) method. The photodetector exhibits a high 3-dB bandwidth of more than 35 GHz and a responsivity of 0.291 A/W at 1550 nm directly coupled with a cleaved fiber. Moreover, a linear response of more than 72-mW optical power is achieved, where a photocurrent of more than 21 mA is obtained at a reverse bias voltage of 3 V.

Keywords: high-performance, diluted waveguide, evanescent coupling, waveguide photodiode

PACS: 85.60.Dw, 42.81.Qb, 73.40.Kp **DOI:** 10.1088/1674-1056/22/10/108503

1. Introduction

Nowadays, the demand for high-speed dense wavelength-division-multiplexing transmission systems and numerous analog and digital optical links is continuously growing. Photodetectors with high bandwidths, high quantum efficiencies, and high-power handling capabilities have become critical components in these systems.[1–4] Among them, side-illuminated waveguide photodetectors attract lots of attention due to their capabilities of overcoming the compromise between quantum efficiency and bandwidth for conventional vertically-illuminated photodetectors.[5–7] However, the disadvantage of conventional waveguide photodetectors is that it is too difficult to obtain high coupling efficiency with a fiber because of a thin coupling cross section.[8] Thus, the evanescently coupled waveguide photodetector (ECWG-PD) with a diluted waveguide which has a multilayer-structure was proposed to solve this problem. Moreover, an important predominance of an ECWG-PD is its excellent high-power handling capability because of the better distribution of generated carriers along the photodiode which relaxes the space charge effect.[9–12]

ECWG-PDs with a short planar multimode waveguide have been reported by several research groups, whose responsivity is enhanced by exploiting the mode beating effects in a multimode waveguide.[3,9,13] Unfortunately, this kind of ECWG-PD is very sensitive to the cleaved waveguide length.[6] In this paper, we design and fabricate another kind of ECWG-PD which comprises a 60-μm-length single-mode rib waveguide, a diluted waveguide, and a p–i–n photodiode with an extended optical matching layer. Due to single-mode transmission in the transmission waveguide without the mode beating effect, this structure has a large tolerance to the cleaved waveguide length and is easy to fabricate and couple with the cleaved fiber.

The experimental results show that our photodetector on one side processes a high 3-dB bandwidth of more than 35 GHz which is much higher than that of the domestic similar device. For example, Zhang *et al.*[14] in 2009 reported a UTC-EC-PD with a 3-dB bandwidth of 11.5 GHz and Zuo *et al.*[3] in 2011 investigated a multimode waveguide EC-PD whose 3-dB bandwidth is 13.4 GHz. On the other side, a linear response of more than 72-mW optical power was achieved, where a photocurrent of more than 21 mA was obtained at 3 V reverse bias voltage. Furthermore, this ECWG-PD is very suitable for the monolithic integration with other components.[1]

2. Design and fabrication

The three-dimensional (3D) schematic structure and cross section of the ECWG-PD operating at 1.55 μm are shown in Figs. 1(a) and 1(b), which mainly comprises a diluted waveguide, a single-mode rib waveguide, and a p–i–n photodiode with an extended optical matching layer. The semi-insulating diluted waveguide is composed of four $InGa_{0.11}As_{0.25}P$ (1.06-μm bandgap) layers, each of which is interspersed between two InP layers. Above the diluted waveguide, there are a semi-insulating $InGa_{0.11}As_{0.25}P$ (520 nm) coupling waveguide layer and a semi-insulating $InGa_{0.11}As_{0.25}P$ (200 nm) single-mode rib waveguide layer which feeds the following p–i–n

*Project supported by the High Technology Research and Development Program of China (Grant Nos. 2012AA012202 and 2013AA031401), the National Basic Research Program of China (Grant No. 2012CB933503), and the National Natural Science Foundation of China (Grant Nos. 61176053, 61274069, and 61021003).

†Corresponding author. E-mail: xhyang@semi.ac.cn

‡Corresponding author. E-mail: hanqin@red.semi.ac.cn

© 2013 Chinese Physical Society and IOP Publishing Ltd

photodiode. The length and width of the rib waveguide are 60 μm and 2 μm, respectively. A 320-nm-thick n^+-doped (Si: 2×10^{18} cm^{-3}) InGaAsP (1.33-μm bandgap) layer, which is grown on the rib waveguide, is used as a low-resistance n-type contact layer. Meanwhile, a 420-nm-thick intrinsic $In_{0.53}Ga_{0.47}As$ absorption layer of the p–i–n photodiode mesa is embedded within the n-contact layer and an upper 410-nm-thick p-doped (Zn: 1×10^{18} cm^{-3}) InGaAsP (1.15-μm bandgap) cladding layer whose refractivity is lower than the absorption layer so as to protect the incident light from being weakened by the metal contact electrodes. Finally, an 80-nm-thick p^+-doped (Zn: 1×10^{19} cm^{-3}) $In_{0.53}Ga_{0.47}As$ is used as a p-contact layer for a good p-type contact. The n-contact layer, which is extended by a protrusion length (L) from the p–i–n mesa also serves as the optical matching layer, providing a refractivity match between the waveguide and the absorption layer. Therefore, the protrusion length L affects the optical intensity distribution in the p–i–n photodiode.[11]

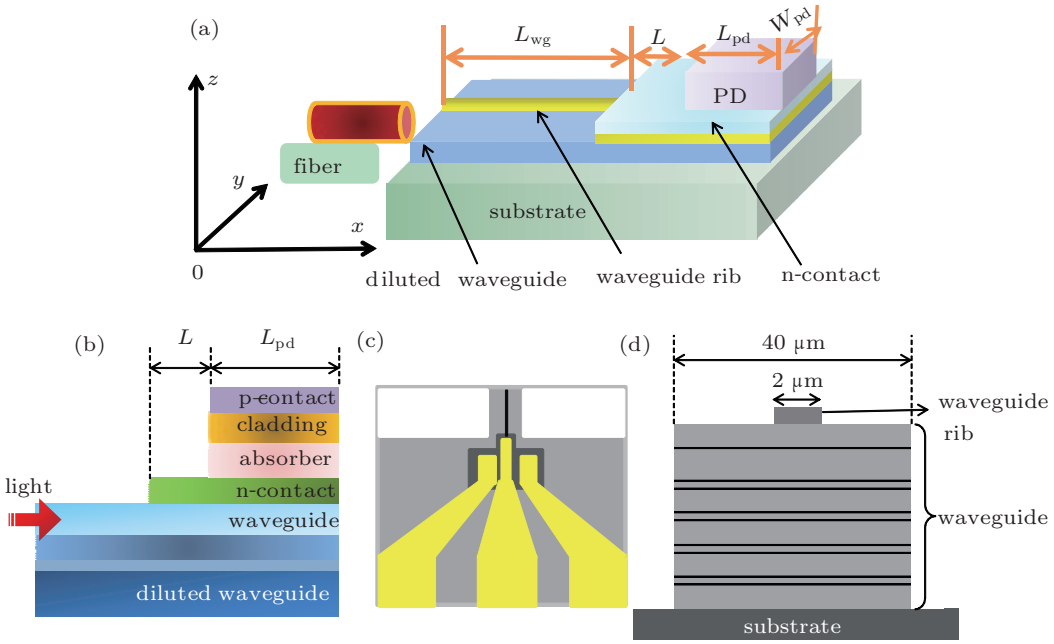


Fig. 1. (color online) (a) The schematic plot of the three-dimensional (3D) simulation structure, (b) the cross section, and (c) the top view of the evanescently coupled waveguide photodetector, and (d) the cross section of the transmission waveguide.

In order to make a good choice of the protrusion length L of the n-contact layer, the optical characteristics of this structure are studied by using professional nano-optical design software — FDTD solutions, using a three-dimensional finite-difference time-domain (3D FDTD) method. The typical simulation results of the absorption efficiency versus photodiode length L_{pd} with different values of matching layer length L are presented in Fig. 2(a), from which one can confirm that the absorption efficiency increases with the photodiode length L_{pd} increasing. For a fixed value of L_{pd}, the absorption efficiency with nonzero matching layer length L is higher than that of $L=0$ [the black squares in Fig. 2(a)]. Especially, taking the case of L_{pd} =20 μm and $L=5$ μm [the green hexagons in Fig. 2(a)] for example, the absorption efficiency is enhanced by 10%. Therefore, for the same absorption efficiency, the area of the PD mesa with nonzero L is smaller than that with $L=0$, which will result in lowered capacitance of the PD and enhanced bandwidth. For instance, if the absorption efficiency is fixed to be 0.22, one can easily get that the area of the PD mesa with $L=5$ μm is 5 μm×8 μm smaller than that with $L=0$ μm, and correspondingly, the capacitance of the PD is reduced by 40%. This is because of the mode beating effects in the multimode waveguide. The matching layer length L-dependent absorption efficiencies for the values of photodiode length $L_{pd}=10, 20$, and 25 are also shown in Fig. 2(b). Obviously, one can find from Fig. 2(b) that with $L_{pd}<20$ μm, the peak absorption efficiency is at $L=5$ μm. As a result, based on these simulated results, the optimized parameters of the p–i–n PD mesa in our proposed device are chosen to be $L=5$ μm and $L_{pd}=20$ μm for further simulations and experiments (see the following text).

The simulated optical intensity as light propagates through the ECWG-PD with $L_{wg}=60$ μm, $L=5$ μm, and $W_{pd}=5$ μm are exhibited in Fig. 3(a). While the images of the simulated field intensity profiles in the single-mode waveguide, multimode waveguide matching layer, and multimode PD mesa are presented in Figs. 3(b), 3(c), and 3(d) respectively. According to the optical field distribution, we can clearly see that the light transmits along the single-mode waveguide and is converted into multimode transmission at the n-contact layer, and then is absorbed by the active layer of the p–i–n PD mesa when the light enters into the PD mesa.

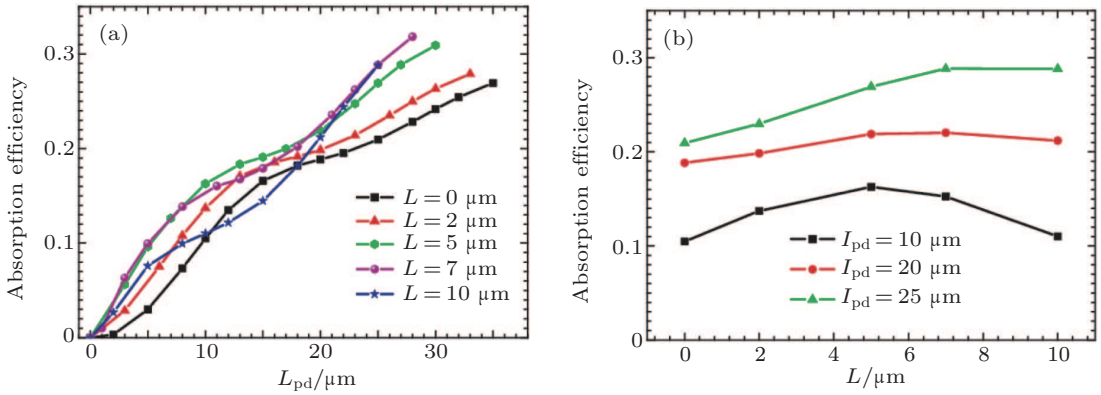


Fig. 2. (color online) (a) Plots of simulated absorption efficiency versus photodiode length L_{pd} with different values of matching layer length $L = 0$, 2, 5, 7, 10 μm. (b) Matching layer length $L =$ dependent the absorption efficiencies for the cases of photodiode length $L_{pd} = 10$, 20, and 25 μm.

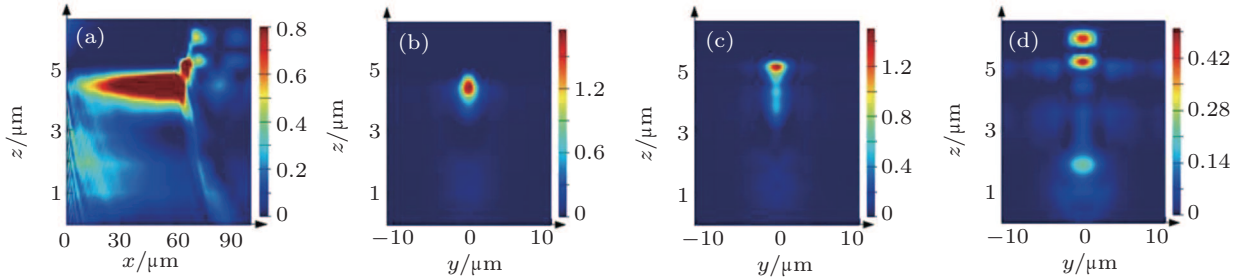


Fig. 3. (color online) (a) Simulated optical intensity as light propagates through the whole device, and (b)–(d) depict the simulated field intensity profiles in the single-mode waveguide, multimode waveguide matching layer, and multimode PD mesa, respectively.

After obtaining these simulation results, the epitaxial structure of the ECWG-PD with the optimized parameters is grown by metal–organic chemical vapor deposition (MOCVD) on semi-insulating InP substrate. Device fabrication is carried out using conventional UV lithography techniques. Firstly, Ti/Au is evaporated and patterned for the p-type contact, which is also employed as mask for the following p–i–n PD mesa etching. The PD mesa (5 μm×20 μm) is successively realized using nonselective wet etching (Br_2:HBr:H_2O) and selective wet etching (H_2SO_4:H_2O_2:H_2O). Then, the larger n-contact mesa and 2-μm-wide rib waveguide are successively fabricated by selective wet etching. After that, Au/Ge/Ni is deposited to form n-contact electrodes. After SiO_2 passivation and contact opening, Ti/Au is evaporated and patterned to form coplanar microwave lines. Finally, two pairs of Ta_2O_5/SiO_2 quarter-wave stacks are grown as antireflection (AR) coating after cleaving.

3. Experimental results and discussion

The current–voltage characteristics of the ECWG-PD is measured using an HP 4140B pA meter. As shown in Fig. 4, the dark currents are 80 pA and 2.1 nA for a PD of 5 μm×20 μm junction area at 0 V and a reverse bias of 3 V, respectively.

Photoresponse measurement is carried out using a 1550-nm laser source and an erbium-doped fiber amplifier (EDFA). The output of the EDFA is coupled to a 9-μm-diameter single mode fiber. The maximal output power of this test system is about 72 mW. The simulated responsivities for various values of p–i–n PD mesa length L_{pd} without AR coating ($L = 5$ μm, PD width = 5 μm) at 1.55 μm are plotted in Fig. 5, see the blue solid circles. The measured responsivity of 0.2 A/W for the 5 μm×20 μm area photodetectors without AR coating (the red rectangle) is slightly lower than the simulation of 0.274 A/W due to the optical loss induced by roughness on the input facet. The measured responsivity for the 5 μm×20 μm area photodetectors with AR coating (the red star) is 0.291 A/W.

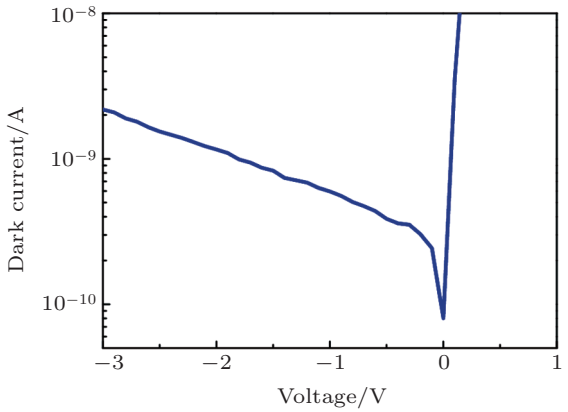


Fig. 4. (color online) The current–voltage characteristic curve of a 5 μm×20 μm ECWG-PD.

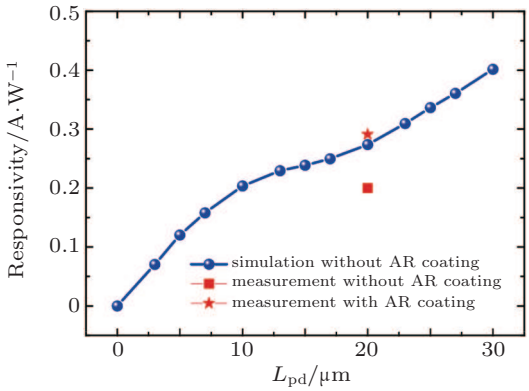


Fig. 5. (color online) Plots of simulated responsivity at 1.55 μm versus p–i–n PD mesa length L_{pd} without AR coating ($L = 5$ μm, PD width=5 μm). The rectangle represents the measured responsivity of the 5 μm×20 μm area photodetectors without AR coating. The star represents the measured responsivity of the 5 μm×20 μm area photodetectors with AR coating.

Figure 6 shows the photocurrent of a 5 μm×20 μm ECWG-PD versus input optical power at 1550 nm under various bias voltages. Under 3-V reverse bias, the ECWG-PD has a linear photoresponse up to 72-mW optical power (the maximal output power of this test system) corresponding to a photocurrent of more than 21 mA. This measurement result indicates that the ECWG-PD has an excellent high-power handling capability. It is very useful to radio over fiber (ROF) system.[3]

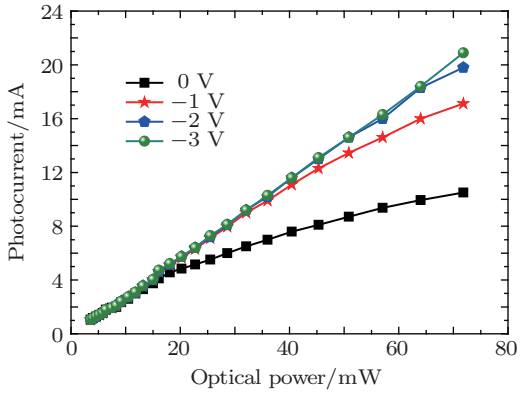


Fig. 6. (color online) Plots of photocurrent of a 5 μm×20 μm ECWG-PD versus input optical power at 1550 nm under various reverse bias voltages.

Our frequency response measurement setup is based on a 1.55-μm DFB-LD and a microwave automatic network analyzer. Figure 7 shows the measured 3-dB bandwidth of a 5 μm×20 μm ECWG-PD at −1 V bias. A 3-dB bandwidth of more than 35 GHz is achieved with a 50-Ω load resistance. According to the typical equations with respect to bandwidth,[15,16] the 3-dB bandwidth $f_{3\ \mathrm{dB}}$ is given by

$$\frac{1}{f_{3\ \mathrm{dB}}^2} \cong \frac{1}{f_{\mathrm{t}}^2} + \frac{1}{f_{\mathrm{RC}}^2}, \tag{1}$$

where the transit-time limited bandwidth and the resistance-capacity (RC) time constant limited bandwidth are expressed as

$$f_{\mathrm{t}} \cong \frac{3.5 \times \bar{v}}{2\pi W}, \tag{2}$$

and

$$f_{\mathrm{RC}} \cong \frac{1}{2\pi C(R_{\mathrm{s}} + R_{\mathrm{L}})}, \tag{3}$$

respectively. Here, $\bar{v}$ denotes the average velocity of the electrons and holes, W is the absorber thickness, C describes the diode capacitance, R_{s} is the series resistance, and R_{L} is the load resistance. The calculated f_{t} is about 70.3 GHz and f_{RC} is 45 GHz based on the measured series resistance of 80 Ω of the PD. Therefore, the theoretical 3-dB bandwidth $f_{3\ \mathrm{dB}}$ should be 39 GHz for this 5 μm×20 μm ECWG-PD without alloying. Obviously, the 3-dB bandwidth is limited by the RC-time constant, owing to the large measured resistance. Thus, if the alloyed condition can be optimized to further reduce the series resistance of the photodetector, the high-frequency performances of the ECWG-PD will be significantly improved.

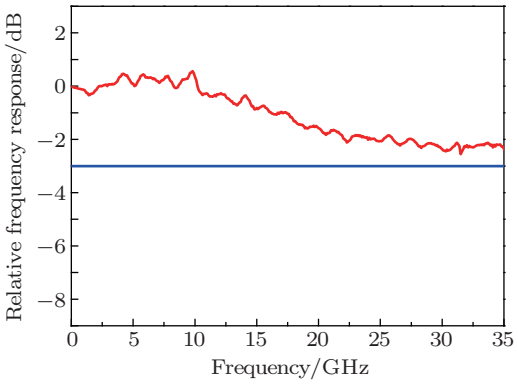


Fig. 7. (color online) Frequency response of a 5 μm×20 μm ECWG-PD at −1-V bias.

4. Summary

In this paper, we report an evanescently coupled waveguide photodetector operating at 1.55 μm. This EC-PD has a large tolerance to the cleaved waveguide length and is easy to fabricate. A high 3-dB bandwidth of more than 35 GHz is measured along with a responsivity of 0.291 A/W at 1550 nm for a 5 μm×20 μm PD. The ECWG-PD has a linear response of more than 72-mW optical power, where a photocurrent of more than 21 mA is obtained at 3-V reverse bias voltage. These measured results are limited by our test system. In addition, the high-frequency performances of the ECWG-PD will be greatly enhanced if the alloyed condition has been optimized to further decrease the series resistance of the photodetector.

References

[1] Beling A and Campbell J C 2009 *J. Lightwave Technol.* **27** 343

[2] Williams K J, Tulchinsky D A and Campbell J C 2007 *IEEE Microwave Photonics (Conference Publications)* **1-4244-1168-8/07** 9

[3] Zuo Y H, Quan C, Zhang Y, Zhang L Z, Guo J C, Xue C L, Cheng B W and Wang Q M 2011 *Chin. Phys. B* **20** 018504

[4] Kato K 1999 *IEEE Microwave Theory Tech.* **47** 1265

[5] Park J W 2010 *IEEE Photon. Technol. Lett.* **22** 975

[6] Wu Y S, Shi J W, Chiu P H and Lin W 2007 *IEEE Photon. Technol. Lett.* **19** 1682

[7] Kato K, Hata S, Kozen A, Yoshida J I and Kawano K 1991 *IEEE Photon. Technol. Lett.* **3** 820

[8] Kato K, Hata S, Kawano K, Yoshida J I and Kozen A 1992 *IEEE J. Quantum Electron* **28** 2728

[9] Achouche M, Magnin V, Harari J, Carpentier D, Derouin E, Jany C, Blache F and Decoster D 2004 *IEEE Photon. Technol. Lett.* **16** 584

[10] Demiguel S, Giraudet L, Joulaud L, Decobert J, Blache F, Jorge V Coupé F, Pagnod-Rossiaux P, Boucherez E, Achouche M and Devaux F 2002 *J. Lightwave Technol.* **20** 2004

[11] Beling A, Bach H G, Mekonnen G G, Kunkel R and Schmidt D 2007 *IEEE J. Sel. Topics Quantum Electron* **13** 15

[12] Zhang Y, Zuo Y H, Guo J C, Ding W C, Cheng B W, Yu J Z and Wang Q M 2009 *Chin. Phys. B* **18** 225

[13] Demiguel S, Li N, Li X W, Zheng X G, Kim J Y, Campbell J C, Lu H F and Anselm A 2003 *IEEE Photon. Technol. Lett.* **15** 1761

[14] Zhang Y X, Liao Z Y and Wang W 2009 *Chin. Phys. B* **18** 2393

[15] Kato K, Hata S, Kawano K and Kozen A 1993 *IEICE Trans. Electron E* **76-C** 214

[16] Achouche M, Magnin V, Harari J, Carpentier D, Derouin E, Jany C and Decoster D 2006 *IEEE Photon. Technol. Lett.* **18** 556